

Beta-delayed proton decay of  $^{61}\text{Ge}$ 

M. A. C. Hotchkis, J. E. Reiff, D. J. Vieira,\* F. Blönnigen,† T. F. Lang, D. M. Moltz, X. Xu, and Joseph Cerny

Department of Chemistry and Lawrence Berkeley Laboratory, University of California, Berkeley, California 94720

(Received 25 August 1986)

The  $T_z = -\frac{3}{2}$ ,  $A = 4n + 1$  nuclide  $^{61}\text{Ge}$  has been produced via the  $^{40}\text{Ca}(^{24}\text{Mg}, 3n)$  reaction and identified by its beta-delayed proton emission. A single proton group at  $3.11 \pm 0.03$  MeV with  $t_{1/2} = 40 \pm 15$  ms has been observed, corresponding to decay of the  $T = \frac{3}{2}$  isobaric analog state in  $^{61}\text{Ga}$  to the ground state of  $^{60}\text{Zn}$ . Searches for the beta-delayed proton decay of the next member of this series,  $^{65}\text{Se}$ , to be produced by the  $^{40}\text{Ca}(^{28}\text{Si}, 3n)$  reaction, have proven unsuccessful.

## INTRODUCTION

The decays of many proton-rich light nuclei have been identified by their beta-delayed proton emission. This work is facilitated by the fact that the isobaric analog state, which is well populated by the superallowed beta transition, is unbound to (isospin forbidden) proton emission. In such cases the overall delayed proton branching ratio is large, and the proton spectra are dominated by transitions from the isobaric analog state to low-lying levels in the proton daughter. All members of the  $T_z = -\frac{3}{2}$ ,  $A = 4n + 1$  series of nuclei from  $^{17}\text{Ne}$  to  $^{57}\text{Zn}$ , and all known beta-decaying  $T_z = -2$  nuclei, exhibit this decay pattern. In the present work we have extended the  $T_z = -\frac{3}{2}$ ,  $A = 4n + 1$  series by observing the delayed proton decay of  $^{61}\text{Ge}$ . Additionally, we have searched for the next member of this series,  $^{65}\text{Se}$ .

Observation of the decays of these nuclei in this mass region provides a means of probing the proton drip line, whose location we have predicted by applying the Kelson-Garvey mass relation.<sup>1</sup> This charge symmetric mass relation requires as input the masses of the  $T_z = +\frac{1}{2}$  and  $-\frac{1}{2}$  nuclei and the mass of the mirror of the nucleus being calculated. For  $A \geq 61$ , the masses of the  $T_z = -\frac{1}{2}$  series are not known, so they have been calculated from their mirror nuclei using a formula for Coulomb displacement energies derived from a recent fit to data.<sup>2</sup> These calculations indicate that the lightest particle stable isotope for each element in this region is expected to be  $^{60}\text{Ga}$ ,  $^{60}\text{Ge}$ ,  $^{66}\text{As}$ ,  $^{65}\text{Se}$ ,  $^{70}\text{Br}$ , and  $^{69}\text{Kr}$ . Lack of mass measurements for the  $T_z = +\frac{1}{2}$  series with  $A > 70$  prevents application of this technique for higher  $Z$  elements. The energies of beta-delayed protons corresponding to the decay of the isobaric analog state in the daughter nuclide can also be estimated in each case, by again applying the Coulomb displacement energy formula, with the calculated mass of the  $T_z = -\frac{3}{2}$  nucleus and the known mass of the proton daughter; hence such measurements provide indirect tests of these mass predictions.

These mass calculations predict that  $^{65}\text{As}$ , the beta daughter of  $^{65}\text{Se}$ , should be unbound to proton emission by  $570 \pm 300$  keV, the uncertainty being dominated by the experimental uncertainty in the mass of  $^{64}\text{Ge}$ ; hence, all

beta decays of  $^{65}\text{Se}$  should lead to proton emission. It is also possible that  $^{65}\text{As}$  is a ground state proton emitter with a measurable lifetime. However, its observation would be experimentally difficult since its half-life may be very short, and the proton energies would be too low for conventional  $\Delta E$ - $E$  silicon detector telescope techniques.  $^{65}\text{As}$  is also of considerable interest for its role in the astrophysical  $rp$  process.<sup>3</sup>

## EXPERIMENTAL METHOD

Beta-delayed proton emitters have been observed among the products of the  $^{24}\text{Mg} + \text{Ca}$  reaction at energies from 77 to 120 MeV and the  $^{28}\text{Si} + \text{Ca}$  reaction from 73 to 128 MeV. The beams were provided by the Lawrence Berkeley Laboratory 88-in. cyclotron. Two different methods were used to observe beta-delayed protons. One setup employed a pulsed beam technique observing radioactive recoils stopped in the target, while the other used a helium-jet transport system. In both cases silicon detector telescopes were used to detect the activities.

In the pulsed beam experiment, the detectors were protected from radiation damage by a rotating tantalum wheel located between the target and the detectors. The slotted wheel controlled the pulsing of the beam, and per-

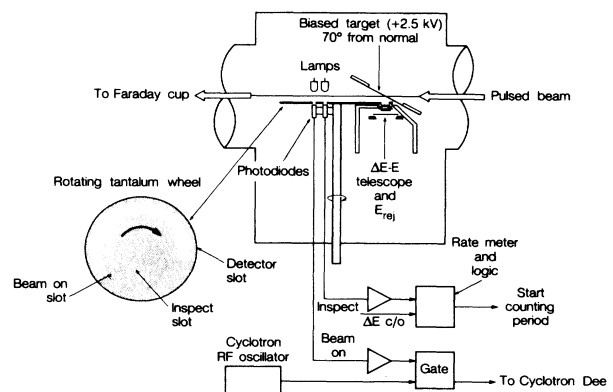


FIG. 1. Diagram of the pulsed-beam target observation system and associated electronics which control the pulsing of the cyclotron beam and initiation of the counting period.

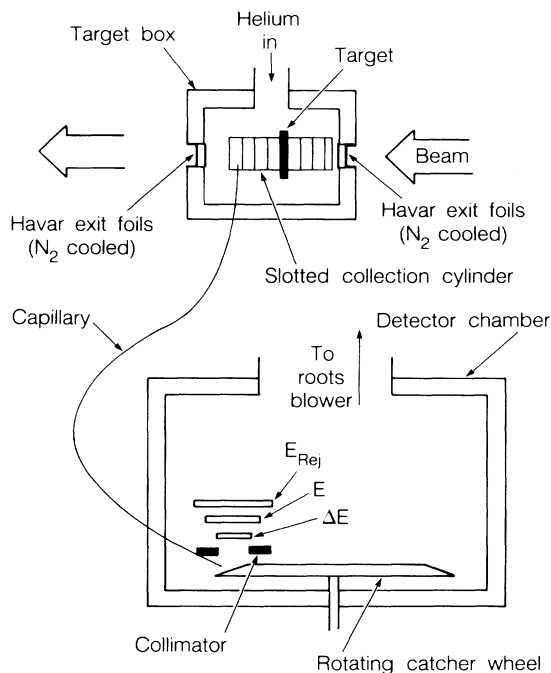


FIG. 2. Schematic diagram of the helium-jet transport system.

mitted the detectors to view the target through a slot in the wheel while the beam was off. The target, biased to +2.5 kV to suppress electron emission, was positioned at an angle of  $20^\circ$  to the beam direction. A detector telescope, which consisted of a  $15\ \mu\text{m}$   $\Delta E$  detector and a  $250\ \mu\text{m}$   $E$  detector, was located perpendicular to the beam and detected protons emitted by products retained in the target, with an effective solid angle of 0.24 sr. A typical timing cycle consisted of an irradiation period of 85 ms with an inspection period of 15 ms (to establish beam cessation) followed by a counting period of 120 ms which was divided into eight 15 ms channels. This setup, identical to that used to discover the beta-delayed proton emission of  $^{53}\text{Ni}$  and  $^{57}\text{Zn}$ ,<sup>4</sup> is shown in Fig. 1. This method was used with 78 and 85 MeV  $^{24}\text{Mg}$  beams incident upon a  $1.5\ \text{mg cm}^{-2}$  natural calcium target. The beam was produced in a Penning ion gauge source and gave beam currents of 20–50 particle nA. Known peaks in the delayed proton spectra of  $^{25}\text{Si}$  and  $^{41}\text{Ti}$ , produced in  $^3\text{He} + \text{Mg}$  and  $^3\text{He} + \text{Ca}$  reactions, respectively, were used to calibrate the detector telescope.

The other experiments employed a helium-jet transport system which is shown schematically in Fig. 2. Nuclei recoiling from a  $1.9\ \text{mg cm}^{-2}$  natural calcium target normal to the beam were thermalized in 1.3 atm of helium. These reaction products were transported on NaCl aerosols through a 70 cm long capillary (1.27 mm i.d.) to a shielded detector box. There they were deposited on the surface of a 15 cm diam rotating disk, directly in front of a three-element silicon detector telescope consisting of  $20\ \mu\text{m}$   $\Delta E$ ,  $272\ \mu\text{m}$   $E$ , and a  $300\ \mu\text{m}$  reject detector. The  $\Delta E$ - $E$  combination permitted the identification of protons

with energies ranging from 1.2 to 6.5 MeV. Calibration of the telescope was achieved using delayed protons from  $^{21}\text{Mg}$ ,  $^{25}\text{Si}$ ,  $^{29}\text{S}$ ,  $^{37}\text{Ca}$ ,  $^{41}\text{Ti}$ , and  $^{45}\text{Cr}$  produced in the  $^{14}\text{N} + \text{Ca}$  reaction at 165 MeV (all listed bombarding energies are “on-target” values). The rotating disk served a dual purpose: (1) it moved long-lived activities away from the detectors, and (2) by using two different disk speeds, qualitative information on the half-lives of the activities was obtained. The overall efficiency of this system is approximately twice that of the target counting method. The beams used in these experiments were produced in an electron cyclotron resonance (ECR) source coupled to the cyclotron; typical beam currents were 100 particle nA for the  $^{24}\text{Mg}$  beams and 100–200 particle nA for the  $^{28}\text{Si}$  beams.

## RESULTS

### $^{24}\text{Mg} + \text{Ca}$

The beta-delayed proton spectrum obtained at 85 MeV from the pulsed-beam target observation technique is shown in Fig. 3. This spectrum is the result of 25 mC of integrated beam (10+) on target. A peak is observed at  $E_{\text{lab}} = 3.10 \pm 0.07\ \text{MeV}$ , which can be attributed to the decay of  $^{61}\text{Ge}$  (see below). At 78 MeV this peak is also evident, with a yield two-thirds of that at 85 MeV. Its half-life was deduced to be  $40 \pm 15\ \text{ms}$  using data from both bombardments; the decay curve is shown in Fig. 4. Peaks at 1.78 and 2.08 MeV, which had long half-lives, are identified as being due to the delayed proton decay of  $^{59}\text{Zn}$  ( $t_{1/2} = 210\ \text{ms}$ ).<sup>5</sup>

Figure 5 shows the delayed proton spectrum obtained with the helium-jet transport system in the 120 MeV bombardment. In addition to a peak at 3.11 MeV, delayed protons from  $^{53}\text{Co}^m$ ,  $^{57}\text{Zn}$ ,  $^{59}\text{Zn}$ , and  $^{25}\text{Si}$  are evident. The yields of the proton groups at this energy have been compared to those at 77 and 90 MeV, also measured with this system. These observations have been compared to calculations made with the statistical model fusion-evaporation code ALICE.<sup>6</sup> The yields of  $^{53}\text{Co}^m$ ,  $^{57}\text{Zn}$ , and  $^{59}\text{Zn}$  were

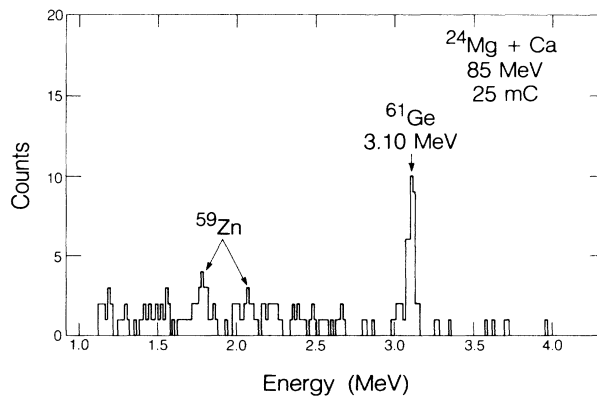


FIG. 3. The delayed proton spectrum from the  $^{24}\text{Mg} + \text{Ca}$  reaction at 85 MeV using the pulsed-beam target observation system.

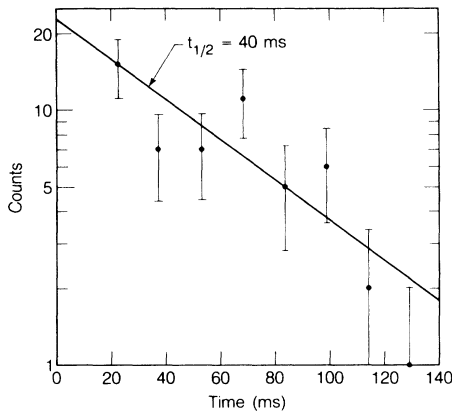


FIG. 4. The decay curve for  $^{61}\text{Ge}$ , incorporating data taken at 78 and 85 MeV.

found to be consistent with these calculations.  $^{25}\text{Si}$  is believed to be produced in transfer reactions on the Havar target chamber entrance foils where the beam energy is sufficiently high (146 MeV) for such reactions to occur. The 3.11 MeV peak is attributed to the decay of  $^{61}\text{Ge}$ , since its yield is a maximum at 90 MeV, as expected from the ALICE calculations. This peak is identified as the transition from the isobaric analog state in  $^{61}\text{Ga}$ , fed by the superallowed beta decay of  $^{61}\text{Ge}$ , to the ground state of  $^{60}\text{Zn}$ . The predicted proton energy for this transition obtained from the Kelson-Garvey mass relation and the Coulomb displacement energy calculations previously mentioned is 3.21 MeV.

Since the energy of the 3.11 MeV peak observed here coincides with that of the dominant group in the delayed proton spectrum of  $^{37}\text{Ca}$ , it has been necessary to evaluate the possibility that  $^{37}\text{Ca}$ , produced in reactions on the small oxygen contamination in the target, could be the source of this activity. The effective threshold for the  $^{16}\text{O}(^{24}\text{Mg},3n)^{37}\text{Ca}$  reaction predicted by the ALICE code is at 95 MeV;  $^{37}\text{Ca}$  may, in principle, contribute to the spec-

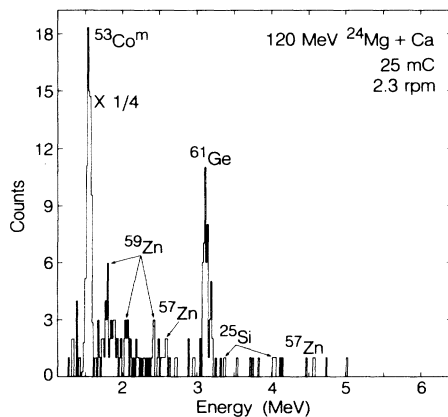


FIG. 5. The delayed proton spectrum from the  $^{24}\text{Mg} + \text{Ca}$  reaction at 120 MeV using the helium-jet transport system.

trum at 120 MeV, but cannot account for the yield of the 3.11 MeV peak being a maximum at 90 MeV and being readily observed at lower energies. Also, the observed half-life of the 3.11 MeV peak is too short for  $^{37}\text{Ca}$  ( $t_{1/2} = 175$  ms). Further evidence against  $^{37}\text{Ca}$  is provided by the data obtained with the  $^{28}\text{Si}$  beam, discussed below, where the peak was again observed while the maximum beam energy was below threshold for the  $^{16}\text{O}(^{28}\text{Si},\alpha 3n)^{37}\text{Ca}$  reaction.

### $^{28}\text{Si} + \text{Ca}$

The  $^{28}\text{Si} + \text{Ca}$  reaction was studied at several energies to search for the delayed proton decay of  $^{65}\text{Se}$ , the next nuclide in the  $T_z = -\frac{3}{2}$ ,  $A = 4n + 1$  series; these experiments also served to confirm the identity of the 3.11 MeV delayed proton peak seen in the  $^{24}\text{Mg} + \text{Ca}$  data. Figure 6 shows two spectra that were obtained with the 128 MeV  $^{28}\text{Si}$  beam. Only the speed of the rotating disk was changed between obtaining these two spectra. The figure shows how the delayed proton peak yields from  $^{53}\text{Co}^m$ ,  $^{61}\text{Ge}$ , and  $^{41}\text{Ti}$  vary with rotation speed. The observed yield of  $^{53}\text{Co}^m$  ( $t_{1/2} = 247$  ms) is clearly suppressed at the faster speed, while those of  $^{61}\text{Ge}$  ( $t_{1/2} = 40$  ms) and  $^{41}\text{Ti}$

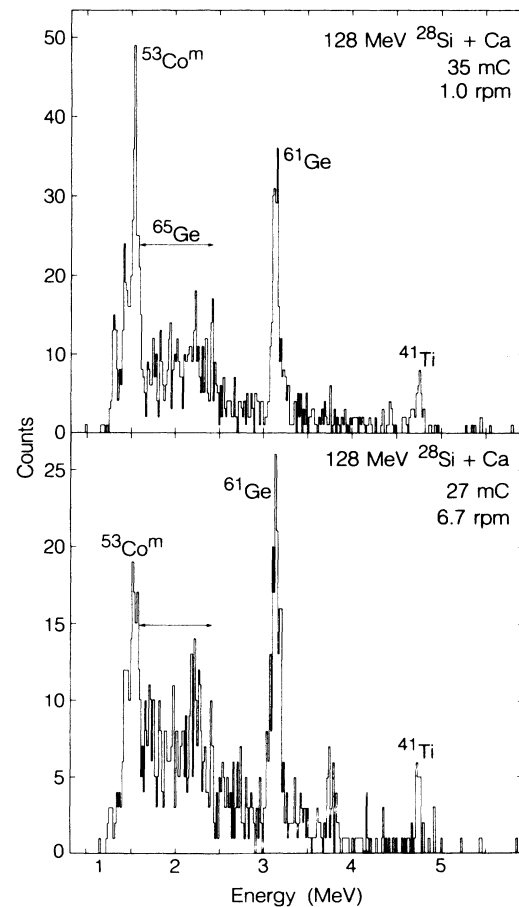


FIG. 6. Delayed proton spectra obtained in the  $^{28}\text{Si} + \text{Ca}$  reaction at 128 MeV with two different disk speeds.

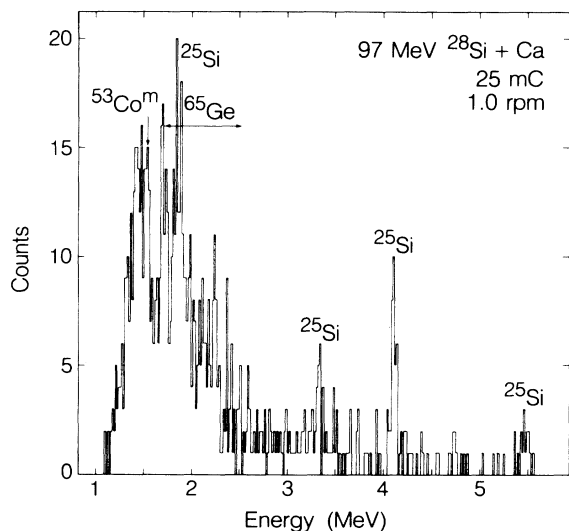


FIG. 7. Delayed proton spectrum from the  $^{28}\text{Si} + \text{Ca}$  reaction at 97 MeV. This is below the threshold for the production of  $^{61}\text{Ge}$ .

( $t_{1/2} = 80$  ms) are not appreciably affected. At the high disk speed, much of the  $^{53}\text{Co}^m$  is removed before decaying, while most of the  $^{41}\text{Ti}$  and  $^{61}\text{Ge}$  nuclei decay while under the detectors.  $^{65}\text{Ge}$  ( $t_{1/2} = 31$  s), produced in the high yield 2pn evaporation channel, emits a continuum of delayed protons ranging from 1.1 to 2.3 MeV;<sup>7</sup> however, the high reaction cross section is offset by its very small proton branch (0.013%).  $^{41}\text{Ti}$  is produced in reactions on the oxygen contaminant in the target. The  $^{61}\text{Ge}$  peak has also been observed in much reduced yield at 113 MeV bombarding energy, but is absent at lower energies, as expected for the 3n evaporation channel.

The spectra in Fig. 6 show no evidence for delayed protons arising from the decay of  $^{65}\text{Se}$ , which has a predicted energy for the transition from the isobaric analog state to the ground state of 3.75 MeV. If the proton decay were to feed either the first or second excited state of  $^{64}\text{Ge}$ , a proton peak at 2.8 or 2.0 MeV would be expected. Since no data are available for  $^{64}\text{Ge}$ , its level scheme has been assumed to be similar to that of  $^{66}\text{Zn}$ , as expected according to the  $N_p N_n$  scheme of Casten.<sup>8</sup>

Figure 7 shows the spectrum obtained when the calcium target was bombarded with 97 MeV  $^{28}\text{Si}$ . This is below threshold for the production of  $^{61}\text{Ge}$ . Present in the spectrum are delayed protons from  $^{53}\text{Co}^m$ ,  $^{65}\text{Ge}$ , and  $^{25}\text{Si}$ . The  $^{25}\text{Si}$  is once again assumed to be produced in transfer reactions off the entrance windows of the target chamber. Again, there is no evidence of protons arising from the decay of  $^{65}\text{Se}$  in this spectrum, or in the data taken at 113 MeV, where its yield is expected to be a maximum. An early attempt to observe  $^{65}\text{Se}$  with the target counting method using the same reaction at 105 MeV was also unsuccessful.<sup>9</sup>

Figures 6 and 7 also show several small peaks superimposed on the  $^{65}\text{Ge}$  continuum, as do data from experiments which used 73 and 81 MeV  $^{28}\text{Si}$  beams. These

peaks, at 1.41, 2.22, and 2.41 MeV, cannot be associated with  $^{65}\text{Se}$  as 81 MeV is below threshold for its production in this reaction. These peaks are believed to arise from the weak beta-delayed proton decays of one or more unknown  $T_z = -\frac{1}{2}$  and  $-1$  nuclei also produced in this reaction. In particular,  $^{60}\text{Ga}$ ,  $^{61}\text{Ga}$ ,  $^{62}\text{Ge}$ ,  $^{63}\text{Ge}$ ,  $^{66}\text{Se}$ , and  $^{67}\text{Se}$  may be contributing. Mass separation would be required to identify the origin of these weak proton groups.

## CONCLUSION

In Fig. 8 a partial decay scheme for  $^{61}\text{Ge}$  is shown, deduced from the results of this work. The beta branching ratio to the isobaric analog state has been estimated assuming  $\log ft = 3.3$  for the superallowed transition. The spins and parities of the ground states of  $^{61}\text{Ge}$  and  $^{61}\text{Ga}$  indicated in Fig. 8 are taken to be the same as in their mirror nuclei. The laboratory energy of the observed delayed proton peak due to  $^{61}\text{Ge}$  is  $3.11 \pm 0.03$  MeV, being the weighted mean of five values obtained in the present experiments; this is in good agreement with the predicted energy of 3.21 MeV for the transition, lending credence to the mass calculations. No evidence has been found in our data of proton decay feeding the first excited state of  $^{60}\text{Zn}$ , which would give rise to a peak at  $E_{\text{lab}} = 2.11$  MeV. An upper limit of 10% of the proton decay can be ascribed to this branch. The mass excess of the lowest  $T = \frac{3}{2}$  state in  $^{61}\text{Ga}$  deduced from this work is  $-43.73 \pm 0.03$  MeV. Since the  $T = \frac{3}{2}$  analog state in  $^{61}\text{Zn}$  is not known, it is not possible to apply the isobaric multiplet mass equation to predict the ground state mass of  $^{61}\text{Ge}$ . Such calculations have been possible for all lighter  $T = \frac{3}{2}$ ,  $A = 4n + 1$  multiplets (see, for example, Ref. 4).

While the uncertainties in the mass predictions do increase farther from stability, our calculations indicate that

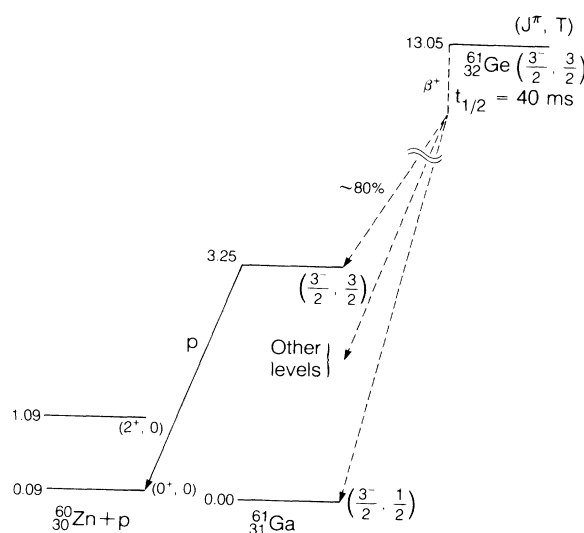


FIG. 8. The proposed decay scheme of  $^{61}\text{Ge}$ . Energies are given in MeV relative to the ground state of  $^{61}\text{Ga}$ . Predicted energies and assumed spins, parities, and isospins are indicated in parentheses.

$^{65}\text{Se}$  should decay by beta emission. It is predicted to be stable with respect to particle decay, with  $S_p = 1.02$  MeV and  $S_{2p} = 0.62$  MeV. Our failure to observe  $^{65}\text{Se}$  may be due to an unexpectedly low cross section for the  $^{40}\text{Ca}(^{28}\text{Si}, 3n)$  reaction. However, according to the ALICE code, the cross section of this reaction is predicted to be about two-thirds of the  $^{61}\text{Ge}$  cross section produced in the

$\alpha 3n$  channel at 128 MeV, so it should have been readily observable in these experiments. Alternatively, it is possible that selenium is not transported efficiently in the helium-jet with NaCl aerosols.

This work was supported by the U.S. Department of Energy under Contract No. DE-AC03-76SF00098.

---

\*Present address: Isotope and Nuclear Chemistry Division, Los Alamos National Laboratory, Los Alamos, NM 87544.

†Permanent address: II Physikalisches Institut, Universität Giessen, Federal Republic of Germany.

<sup>1</sup>I. Kelson and G. T. Garvey, *Phys. Lett.* **23**, 689 (1966).

<sup>2</sup>M. S. Antony, J. Britz, and A. Pape, *At. Data Nucl. Data Tables* **34**, 279 (1986).

<sup>3</sup>The  $rp$  process is effectively terminated at  $^{64}\text{Ge}$  if  $^{65}\text{As}$  is unbound, as it almost certainly must be at the temperature considered for the process ( $\sim 10^9$  K). See S. E. Woosley, in *Proceedings of the Accelerated Radioactive Beams Workshop*, edited by L. Buchmann and J. M. D'Auria (Parkville, Canada, 1985), p. 4.

<sup>4</sup>D. J. Vieira, D. F. Sherman, M. S. Zisman, R. A. Gough, and J. Cerny, *Phys. Lett.* **60B**, 261 (1976).

<sup>5</sup>J. Honkanen, M. Kortelahti, K. Eskola, and K. Vierinen, *Nucl. Phys.* **A366**, 109 (1981).

<sup>6</sup>M. Blann and J. Birplinghoff, Lawrence Livermore National Laboratory Report No. UCID-19614, 1982 (unpublished).

<sup>7</sup>J. C. Hardy, J. A. Macdonald, H. Schmeing, T. Faestermann, H. R. Andrews, J. S. Geiger, R. L. Graham, and K. P. Jackson, *Phys. Lett.* **63B**, 27 (1976).

<sup>8</sup>R. F. Casten, *Phys. Rev. C* **33**, 1819 (1986).

<sup>9</sup>D. J. Vieira, Ph. D. thesis, Lawrence Berkeley Laboratory Report No. LBL-7161, 1978 (unpublished).

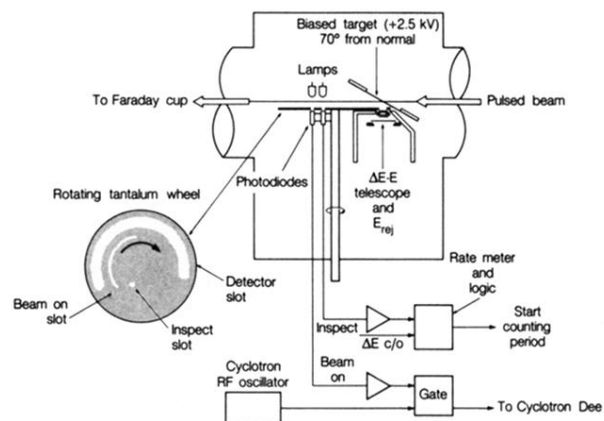


FIG. 1. Diagram of the pulsed-beam target observation system and associated electronics which control the pulsing of the cyclotron beam and initiation of the counting period.